

A seismic monitoring approach to detect and quantify river sediment mobilisation by steelhead redd-building activity

Michael Dietze, GFZ German Research Centre for Geosciences, Section 4.6 Geomorphology, Potsdam, Germany (mdietze@gfz-potsdam.de),

James Losee, Washington Department of Fish and Wildlife, Olympia, Washington, USA (James.Losee@dfw.wa.gov),

Lina E. Polvi, Department of Ecology and Environmental Science, Umeå University, Umeå, Sweden (lina.polvi@umu.se),

Daniel Palm, Department of Wildlife, Fish and Environmental Studies, Swedish University of Agricultural Sciences, Umeå, Sweden (Daniel.Palm@slu.se)

Abstract

The role of spawning salmonids in altering river bed morphology and sediment transport is significant yet poorly understood. This is due, in large part, to limitations in monitoring the redd-building process in a continuous and spatially extended way. A complimentary approach may be provided through the use of a small seismic sensor network analyzing the ground motion signals generated by the agitation of sediment during the redd building process. We successfully tested the viability of this approach by detecting and locating artificially-generated redd signals in a reach of the Mashel River, Washington State, USA. We then utilize records of 17 seismic stations, in which we automatically detected seismic events that were subsequently manually checked, yielding a catalogue of 45 potential redd-building events. Such redd-building events typically lasted between one and twenty minutes and were comprised of a series of clusters of 50–100 short energetic pulses in the 20–60 Hz frequency range. The majority (> 90 %) of these redd building events occurred within eleven days, predominantly during the early morning and late afternoon. The seismically derived locations of the signals were in agreement with independently mapped redds. Improved network geometry and installation conditions are required for more efficient detection, robust location and improved energetic insights to redd building processes in larger reaches. The passive and continuous nature of the seismic approach in detecting redds and describing fish behavior provides a novel tool for fish biologists and fisheries managers, but also for fluvial geomorphologists, interested in quantifying the amount of sediment mobilised by this ecosystem engineer. When complemented with classic approaches, it could allow for a more holistic picture of the kinetics and temporal patterns (at scales from seconds to multiple seasons) of a key phase of salmonid life cycles, with potential implications for biology, ecology, and fluvial geomorphology.

This paper is the second, revised version of a peer reviewed preprint uploaded to EarthArXiv, and submitted to "Earth Surface Processes and Landforms".

Potsdam, 12 June 2020

1 **A seismic monitoring approach to detect and quantify**
2 **river sediment mobilisation by steelhead redd-building**
3 **activity**

4 **M. Dietze¹, J. Losee², L.E. Polvi³, D. Palm⁴**

5 ¹GFZ German Research Center for Geosciences, Section 4.6 Geomorphology, Potsdam, Germany, Tel.:

6 +49 331 288 288 27

7 ²Washington Department of Fish and Wildlife, 600 Capitol Way N. Olympia, Washington, USA, 98501

8 ³Department of Ecology and Environmental Science, Umeå University, 901 87 Umeå, Sweden

9 ⁴Department of Wildlife, Fish and Environmental Studies, Swedish University of Agricultural Sciences,

10 901 83 Umeå, Sweden

11 **Key Points:**

- 12 • Environmental Seismology
13 • Ecosystem Engineers
14 • Salmonid Spawning
15 • Gravel-bed Rivers
16 • Biogeomorphology

Abstract

The role of spawning salmonids in altering river bed morphology and sediment transport is significant yet poorly understood. This is due, in large part, to limitations in monitoring the redd-building process in a continuous and spatially extended way. A complementary approach may be provided through the use of a small seismic sensor network analysing the ground motion signals generated by the agitation of sediment during the redd-building process. We successfully tested the viability of this approach by detecting and locating artificially-generated redd signals in a reach of the Mashel River, Washington State, USA. We then utilize records of 17 seismic stations, in which we automatically detected seismic events that were subsequently manually checked, yielding a catalogue of 45 potential redd-building events. Such redd-building events typically lasted between one and twenty minutes and were comprised of a series of clusters of 50–100 short energetic pulses in the 20–60 Hz frequency range. The majority (> 90 %) of these redd-building events occurred within eleven days, predominantly during the early morning and late afternoon. The seismically derived locations of the signals were in agreement with independently mapped redds. Improved network geometry and installation conditions are required for more efficient detection, robust location and improved energetic insights to redd-building processes in larger reaches. The passive and continuous nature of the seismic approach in detecting redds and describing fish behaviour provides a novel tool for fish biologists and fisheries managers, but also for fluvial geomorphologists, interested in quantifying the amount of sediment mobilised by this ecosystem engineer. When complemented with classic approaches, it could allow for a more holistic picture of the kinetics and temporal patterns (at scales from seconds to multiple seasons) of a key phase of salmonid life cycles.

1 Introduction

In the form of ecosystem engineers or bioturbators, biota can have significant effects on physical earth surface processes (Viles, 1988). Examples include biological weathering (de Oliveira Frascá & Del Lama, 2018), slope stabilization by vegetation (Phillips et al., 2016) and river bank destabilization by invading species (Harvey et al., 2019). Within rivers, ecosystem engineers and bioturbators serve both to trap sediment and reduce erosion, such as beaver and riparian plants stabilizing stream banks, and to increase erosion and sediment transport, such as grazing animals and crayfish (Polvi & Sarneel, 2018). While many of these examples are easily detectable and can be surveyed continuously, some biotically-driven causes of sedimentation or erosion are much harder to constrain using traditional methods, and only their resulting effects can be surveyed. For example, nest building in riverine systems by salmonids is a process that affects river bed sediment movement (Gottesfeld et al., 2004; Hassan et al., 2008) but is rarely monitored in real time.

Salmonid spawning includes building a nest, known as a redd, where eggs are placed and incubated until emergence. The process of redd construction includes the rapid movements of the caudal fin by the female, which agitates the bed material and ultimately transports sediment from a site to excavate a pit. The entire redd-building process has been shown to take up to five days (Burner, 1951) but detailed information on this process is limited. After the initial pit has been excavated, the female deposits eggs in the pit where they are fertilized by one or more males (Quinn, 2018). The eggs are then buried by the female through additional excavation upstream of the pit. Depending on the species, the spawning event and associated redd construction involves the excavation of a significant amount of gravel- and cobble-sized sediment. Specifically, the total length of a redd ranges from 0.31 m to greater than 3 m depending on stream dynamics, species and size of the female (Burner, 1951; Losee et al., 2016). For example, S. Gallagher and Gallagher

67 (2005) documented redds for the anadromous form of *Oncorhynchus mykiss* also known
68 as steelhead, averaging 0.72 m in length.

69 The process of redd building by salmonids has been associated with the removal
70 of benthic organisms (Field-Dodgson, 1987) and sediment transport consistent with that
71 observed during flood events (Gottesfeld et al., 2004). For example, Hassan et al. (2008)
72 found in a selection of small North American streams that in years with low-recurrence
73 interval snow melt floods, redd building by salmonids transported as much sediment as
74 fluvial processes. In years of high flows and dynamic flooding events, salmonids may not
75 directly transport as much sediment as natural fluvial processes but serve to enhance sed-
76 iment mobility by reducing armouring (Hassan et al., 2008). As scarce as such empir-
77 ical evidence currently may be, they illustrate that an important consequence of redd-
78 building can be an altered river bed morphology, by increasing the diversity in river bed
79 morphology, generating a deposit protruding from the riverbed, decreasing armouring
80 and decreasing the degree of particle imbrication (e.g. Rennie & Millar, 2000; Hassan
81 et al., 2008). Over geological time scales, this may alter longitudinal profiles of rivers and
82 increase the erosion efficiency of the entire catchment (Fremier et al., 2018). On the con-
83 trary, a biologically induced increase of bed roughness may also result in reduced shear
84 stress. In summary, the medium- to long-term effect of salmonid-induced river bed re-
85 organization is uncertain given the limited number of quantitative studies on this topic,
86 leading only to idealized formulation approaches in long-term models (e.g. Fremier et
87 al., 2018).

88 Likewise, detailed information on the timing and duration of redd-building activ-
89 ity is unknown. Traditionally, biologists and fisheries managers have relied on the visual
90 identification and enumeration of salmonid redds to determine spawning stock biomass
91 and spawn timing. This work is done through regular monitoring activities, involving
92 one or more stream surveyors visually identifying, enumerating and marking spawning
93 sites every seven to ten days (S. P. Gallagher et al., 2007; Madel & Losee, 2016). Apart
94 from constraining the creation within the lapse time of surveys, retrospective mapping
95 (e.g. Losee et al., 2016) has been used to provide detailed information on the morphol-
96 ogy and geometric properties of the redd but provides limited information regarding the
97 timing of redd construction, duration of spawning events and other behavioural char-
98 acteristics. More detailed information associated with redd-building activity has emerged
99 through selected snorkel surveys (e.g. Rand & Fukushima, 2014), and laboratory stud-
100 ies (Needham & Taft, 1934; Berejikian et al., 2008). These approaches have the advan-
101 tage of delivering direct high resolution information on the fish’s activity during spawn-
102 ing but are limited to daylight or very simplified conditions. Together, none of the ex-
103 isting approaches have been shown to provide a continuous, high resolution and spatially
104 extended record of redd-building activity in a given reach of a river.

105 An alternative and potentially complementary approach to detect, describe and enu-
106 merate spawning sites may be provided by environmental seismology, an emerging re-
107 search field that investigates the seismic signals emitted by Earth surface processes. Mod-
108 ern seismic sensors like geophones or broadband seismometers are sensitive enough to
109 detect processes that emit only minimal impact energy to the ground, such as falling rain
110 drops and wind turbulence (Turowski et al., 2016; Dietze et al., 2017), or rock and ice
111 crack signals (Polvi et al., in review). Seismic sensors have already been used to study
112 sediment mobilization in rivers (Burtin et al., 2016; Schmandt et al., 2017), a process
113 which is inherently difficult to constrain under natural conditions due to the infrequent
114 occurrence of transport, often under hostile flow conditions. There, sediment particles
115 impacting the river bed emitted seismic signals with a characteristic spectral signature,
116 and these signals could be inverted for the mass of sediment that is moving through the
117 river’s cross section at a given time interval (e.g. Dietze, Lagarde, et al., 2019).

118 In this study, we use a small seismic network in an important steelhead (*Oncorhynchus*
119 *mykiss*) spawning area, the Mashel River, Washington State, USA, to investigate whether

120 the redd-building process of steelhead can be detected and located using seismic signals.
121 We also aim to describe fine-scale temporal and spatial patterns of redd construction from
122 observed seismic signals.

123 **2 Study site and instrumentation**

124 The Mashel River is a tributary of the Nisqually River, which originates from the
125 Nisqually Glacier on the slopes of Mt. Rainier and drains 1,890 km² of the western slope
126 of the Cascade Mountain Range. Our study reach was approximately 150 m long on a
127 2nd order stream segment of the Mashel River. Bankfull width ranged from approximately
128 25–70 m and average bed slope was 0.0005 m/m. The sediment size distribution was fairly
129 well sorted, composed of coarse gravel to cobbles, with a D₁₆ of 19.4 mm, D₅₀ of 55.1
130 mm, and D₈₄ of 123.1 mm. This reach was chosen based on the high density of steelhead
131 spawners in past years relative to other parts of the Mashel River. To relate seismic sig-
132 nals to environmental conditions, we used daily meteorological data (NOAA, 2020) and
133 15-min discharge data (USGS, 2020).

134 We deployed 17 seismic stations on land on the left and right banks, approximately
135 2–5 meters from the bank, except for four stations (Fig. 1 a) that were placed at greater
136 distance to explore the spatial range of river-derived signals. Stations were installed with
137 an average spacing of 25 m (average river width) as an irregular network. Since we did
138 not know the ideal network design for the type of signals we recorded, we chose this setup
139 based on pragmatic decisions. The installed stations consisted of PE6B 4.5 Hz vertical
140 component geophones and Digos DataCube data loggers recording at 400 Hz. The spike-
141 equipped sensors were pushed into the ground and the loggers were placed next to the
142 sensor. For longer term installations, one would either place the sensors in pits or cover
143 them with sediment to shield them from atmospheric signals. However, due to the amount
144 of sensors and time constraints this was not possible in this study. The system was equipped
145 with internal batteries, allowing for up to 2 weeks of continuous operation and maintained
146 with fresh batteries for the life of the study (approximately 4 weeks). The stations were
147 deployed on 29 April 2019 and dismantled on 27 May 2019. To constrain essential seis-
148 mic ground properties, we performed an active seismic survey. For this, a metal plate
149 (25 x 10 cm) was placed directly next to individual seismic stations and signals were in-
150 duced by ten subsequent blows with a 5 kg sledge hammer.

151 The potential spectral properties of the redd-building process were inspected by
152 manually mimicking redd-building activities, using three different approaches, for approx-
153 imately one minute each: 1) In the first approach, a person created a hydraulic jet that
154 entrained sediment by intensively flipping a rubber diving fin with its hands. 2) The bed
155 material was moved around at the same site with a boot. 3) Finally, the bed material
156 was gently agitated with a stiff paddle, again without touching the sediment. Before and
157 after each experiment, we exerted a sequence of three hits with a hammer onto a boulder
158 at the left bank of the river to identify each experiment’s start and end time.

159 The study area was visited at regular intervals and manually surveyed for new redd
160 features (26 April, 08 May, 13 May, and 23 May 2020). The same two trained survey-
161 ors were responsible for identifying redds for the duration of the study. Surveyors wore
162 polarized glasses and recorded locations of steelhead redds using standardized survey method-
163 ology (Madel & Losee, 2016). As mentioned above, redds that are constructed by salmonids
164 typically include a well-defined depression (pit) immediately upstream of a mound (tail
165 spill). These features are also identifiable as being absent of macrophytes. Each redd was
166 flagged with the date, the surveyor’s initials, and other descriptive details as needed to
167 avoid double-counting redds. Additionally, coordinates of redd locations were recorded
168 using a hand-held GPS. We assumed that all observed redds were created by steelhead;
169 this was based on several factors: 1) the absence of other salmonids during the sampling
170 period; 2) the observed presence of adult steelhead; and 3) the relatively large size of ob-

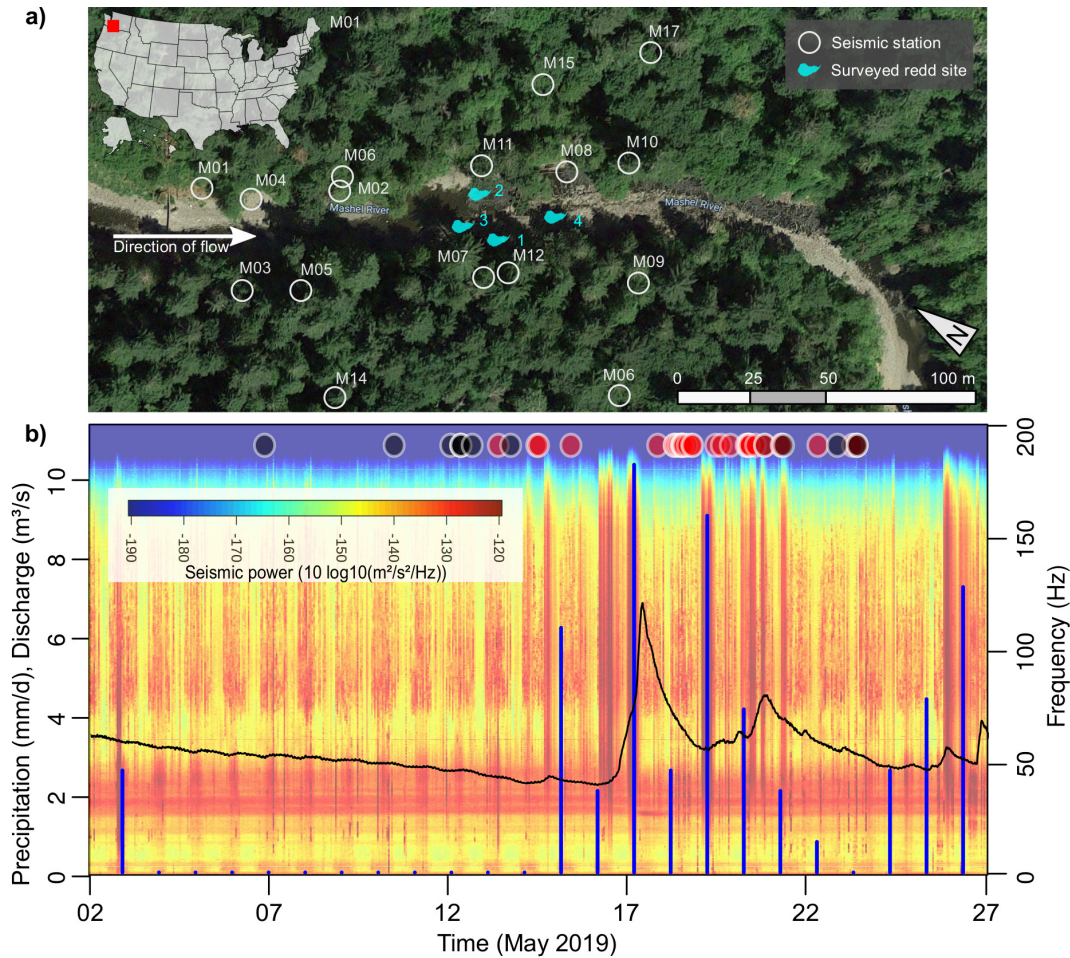


Figure 1. Study area with instrumentation scheme and environmental data. a) The 150 m long straight reach of the Mashel River, Washington State, USA, was instrumented by 17 seismic stations. Redd sites (blue polygons) found during periodic mapping campaigns are located inside the seismic network. Aerial image source: Google Maps. b) Precipitation (blue bars, NOAA station Mayfield Power Plant) and discharge data (black line, station USGS no. 12087000) for the instrumented period. Circles at the top depict manually identified seismic events; black circles are regular events, red circles are events only recorded at station M11, cf. Tab. 1 for details. Background shows a seismic spectrogram of the full period as recorded by station M11.

171 served redds relative to those of other redd-building species potentially present (cutthroat
 172 trout *Oncorhynchus clarkia clarkii* and Pacific Lamprey *Entosphenus tridentatus*).

173 3 Data processing

174 All seismic data were processed with the R package *eseis* v 0.6.0 (Dietze, 2018a,
 175 2018b). The SI contain dedicated R scripts of all major processing and analysis steps.
 176 Seismic data were also interactively visualised using the software *Snuffler* v. 2018.1.29
 177 (Heimann et al., 2017). Raw measurement files were converted from the Cube logger data
 178 format to hourly files (SAC format, IRIS, 2017), organised in a coherent structure (see
 179 SI).

180 To identify discrete events from the continuous stream of ground motion data, we
181 applied a classic STA-LTA trigger algorithm (Allen, 1982), which is sensitive to sudden
182 rises in ground motion amplitudes. We applied this algorithm to hourly signal snippets
183 of all analysed stations, overlapping by 5 minutes on both sides. Hourly snippets (400
184 times 3600 samples) turned out to be ideal in terms of computer memory balance, and
185 the overlap guaranteed that we did not miss events at the snippet margins. The signals
186 were detrended, filtered between 10–20 Hz (window showing the least spectral overlap
187 with the river as constant seismic source) and envelopes, representing hull functions of
188 the signals, were calculated (see SI for code and details). For the subsequent STA-LTA
189 algorithm, we used a short time window of 0.5 s, a long time window of 180 s, an on-ratio
190 of 5 and an off-ratio of 1. The window sizes were based on the assumption that poten-
191 tial events would show a rapid and impulsive onset and would not last longer than three
192 minutes. Since the algorithm usually detects many spurious events, we removed all picks
193 with durations less than 0.2 s and longer than 5 min to ensure that signals were not spu-
194 rious and represented gravel transport results from fish movement. Events shorter than
195 0.2 s are usually spurious instantaneous spikes (Dietze et al., 2017), whereas events longer
196 than a few minutes are caused by earthquakes or anthropogenic sources such as trains
197 or, especially in this particular study, planes (see results). Furthermore, we removed events
198 that were not recorded by at least three stations and within a joint occurrence time win-
199 dow of 1 s, because signals must be detected by at least three stations in order to locate
200 the signal source. The seismic wave velocity in loose sediment is typically a few hundred
201 m/s (Bourbie et al., 1987); therefore, for a maximum distance of 167 m across the utilised
202 network, a seismic wave from a source to a station requires less than 1 s.

203 In order to identify potential redd-building events, all remaining events were checked
204 manually for consistency and validity. Checks were based on the following criteria: 1)
205 presence of short pulses, forming clusters of activity that lasted less than one minute (Needham
206 & Taft, 1934), 2) absence of systematically increasing and decreasing amplitudes, indica-
207 tive of approaching and passing terrestrial animals, including humans, 3) absence of dis-
208 tinct arrivals of seismic phases, indicative of earthquakes; and 4) absence of gliding fre-
209 quency bands (e.g. Fig. 3 a), typical for planes. These criteria were investigated both
210 by studying the raw seismic waveforms interactively and by computing spectrograms,
211 plots of the time evolution of seismic power spectra. The spectrograms were computed
212 using the sub/window averaging technique (Welch, 1967) of deconvolved signals (see SI).

213 The manually-validated events were located using the signal migration technique
214 (Dietze, 2018b). This approach makes use of the finite wave velocity of seismic signals
215 and calculates the relative travel time delay of signals between all possible station pairs.
216 In a grid search procedure, all potential locations (raster pixels) are tested for their po-
217 tential time delays for the same station pairs. The final source location is provided as
218 a density function of the average difference between empirical and pixel-specific poten-
219 tial time delay. The signal migration routine was based on the deconvolved, 10–20 Hz
220 filtered, tapered signal envelopes. Only events with a signal-to-noise ratio (SNR) greater
221 than 3 and recorded by at least three stations were located, using the apparent seismic
222 wave velocity as constrained by the active seismic survey (see below). The resulting lo-
223 cation estimates were truncated to values greater than the quantile $q_{0.99}$, a usual value
224 to define the range of location uncertainty, approximately 10–20 % of the inter-station
225 distance (e.g., Dietze et al., 2017).

226 The average apparent seismic wave velocity was determined by the active seismic
227 survey. The time differences between blows as recorded on the closest station and all other
228 stations were determined by cross correlation of the signal envelopes and converted to
229 a velocity using the distance of each station to the one closest to the hammer blows.

230 4 Results

231 4.1 Mapped redd locations

232 During the study period, surveyors identified a total of four completed redds within
 233 the study reach (Fig. 1 a): redd no. 1 was mapped by 08 May, redd no. 2 by 13 May and
 234 redds no. 3 and no. 4 by 23 May. All new redds identified during the study period were
 235 within 5 m of the left bank. In addition, redd no. 2 showed signs of some fresh digging
 236 in between survey dates as the flag we used to mark it had been slightly covered up with
 237 fresh sediment. Redd size, shape and sediment composition (coarse gravel and cobbles)
 238 were consistent characteristics from other steelhead spawning sites (S. P. Gallagher et
 239 al., 2007).

240 4.2 Environmental conditions during experiment

241 During the first half of the survey period, the Mashel River showed a steadily de-
 242 creasing discharge with minor diurnal fluctuations (Fig. 1 b). From 15 May until the end
 243 of the study period, there were several multi-hour long periods of rain, causing distinct
 244 flashy peaks of the river discharge. The rain events were visible in the seismic spectra
 245 (Fig. 1 b) as broadband bursts of high energy. The sub-minute resolution of the seismic
 246 data also showed that the rain events did not cover an entire day but only a few hours.
 247 The seismic waveforms further showed the typical signature of repeated raindrop impacts:
 248 numerous < 0.2 s long single 20–200 Hz pulses (cf. Dietze et al., 2017). The rain-driven
 249 high flows did not show up visually in the seismic spectrogram, neither as a clear power
 250 increase of the persistent 25–50 Hz band nor as a prominent broadband (20–70 Hz) sig-
 251 nal indicative of bedload transport (cf. Fig. 2 b and Dietze, Lagarde, et al. (2019)). Like-
 252 wise, we saw no indications of recent over bank flooding conditions during our site vis-
 253 its.

254 4.3 Artificial redd-building signal properties

255 The seismic signatures of our three artificial redd-building experiments (Fig. 2) showed
 256 the effects of the applied mechanisms. Type 1 (fin movement causing pebble agitation)
 257 and type 2 (moving sediment with boot) both generated seismic signals more than 10
 258 dB above background, peaking at 25–40 Hz (Fig 2 a). However, the type 2 mechanism
 259 generated a stronger broadband signal overall, approximately 7–8 dB higher than type
 260 1 between 50 and 150 Hz. The type 3 mechanism (contactless pebble agitation with stiff
 261 paddle) only marginally exceeded the background level (blue versus grey curve in Fig. 2 a).
 262 Overall, all three agitation types show similar spectral peaks as the background signal
 263 space.

264 We seismically located distinct amplitude peaks in the signal sequences to test how
 265 well the positions of artificial redd-construction activities can be estimated. Locations
 266 of the sequences of three hits with a hammer onto a boulder prior to the actual redd ex-
 267 periments (Fig. 2 c) deviated from the true site by $3.0^{+0.4}_{-0.2}$ m (median and quartile range).
 268 Two randomly chosen 2–3 s intervals during the type 1 and type 2 redd-construction ex-
 269 periments could also be located with deviations $2.5^{+0.1}_{-0.3}$ m. For the hammer blow signals,
 270 we were able to use a narrow filter frequency window of 16–20 Hz, focusing on frequen-
 271 cies below the river induced signals (Fig. 2 b). For the weaker redd-building experiment
 272 signals, we needed to use a wider frequency window of 16–25 Hz to allow for a sufficient
 273 signal to noise ratio. The active seismic survey yielded an apparent seismic wave veloc-
 274 ity of 350 ± 40 m/s. We used the average value for further analyses. For details on the
 275 results see the SI.

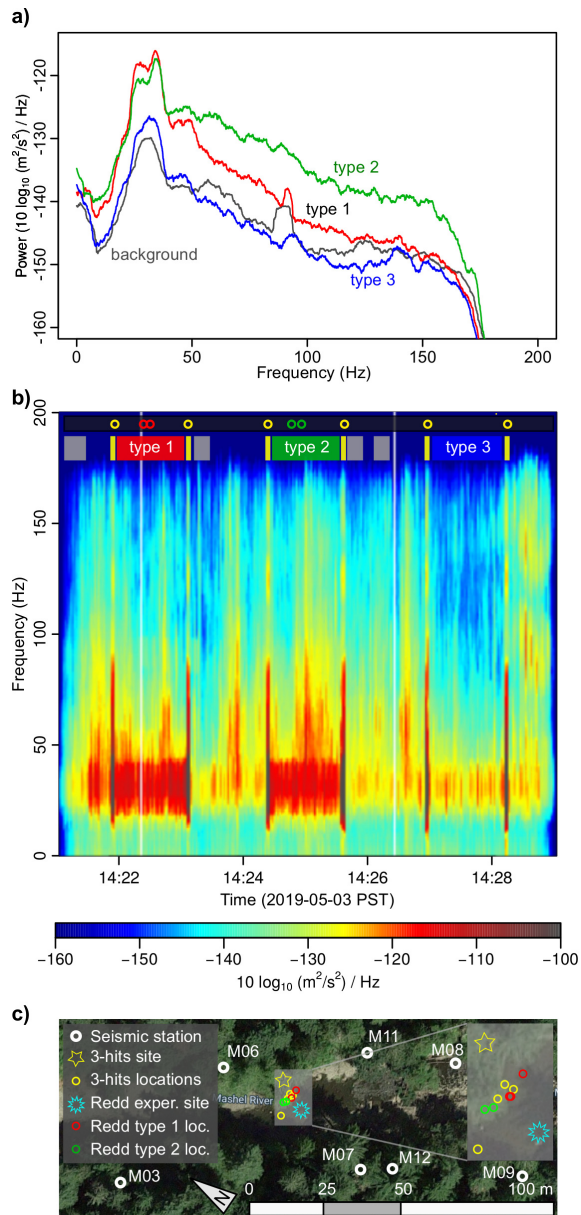


Figure 2. Artificial redd construction experiment signatures. a) Seismic spectra of the three different redd-building approaches and background spectrum. Colour code also used in other panels. b) Spectrogram of the full artificial redd-building sequence, recorded by station M07. Note how three hits with a cobble on a boulder (yellow bars in top part legend) initiate the actual experiments (red, green and blue bars denoting the three types). Dots above top legend indicate time sections used for location of signals. c) Location results of selected event periods as denoted in b). Inset shows enlarged version of the location results. Experiment start and end times were indicated by three hits on a boulder located as indicated by yellow star. The redd-building experiment locations are indicated by the blue star and the seismic location results are depicted by coloured circles.

276 4.4 Event signal characteristics

277 The STA-LTA routine yielded several thousand potential events, of which most were
 278 rejected automatically. We manually checked the remaining 591 potential events using
 279 the software Snuffler. These checks were based on a joint observation of the signals recorded
 280 by stations closest to the independently mapped redd locations (M07, M08, M10, M11
 281 and M12), as well as spatially adjacent stations if these helped to clarify expected am-
 282 plitude reductions and signal arrival time delays with increasing spatial distance from
 283 the potential source.

284 Checks included the criteria defined in section 3. We checked the properties of in-
 285 dividual seismic pulses, including durations, amplitudes and amplitude differences, the
 286 pauses between the pulses, and the evolution of pulse properties throughout the entire
 287 duration of a potential redd-building signature, which is composed of a series of individ-
 288 ual pulses. Most individual signals were clearly visible above background at 3–4 stations,
 289 depending on the amplitudes of individual pulses (see for example Fig. 3 b). Whenever
 290 possible (i.e., a viable signal was recorded by at least three stations), we located the seis-
 291 mic source of individual pulses and rejected a pulse sequence if at least 10 % of the vis-
 292 ible pulses could not be located consistently at the same position within the river chan-
 293 nel (i.e., overlapping location estimates within the 99 % polygon). In total, we identi-
 294 fied 45 potential redd-building signal sequences from 29 April through 27 May.

295 We use one example period (Fig. 3) to illustrate the characteristics of signals in-
 296 dicative of redd-building activities (Fig. 4). After several hours without any short-pulsed
 297 signals, station M11 recorded a series of 256 mostly high-amplitude signals ($\pm 50 \mu\text{m/s}$),
 298 lasting $0.33_{-0.11}^{+0.13}$ s each. The entire phase lasted approximately 12 min and exhibited four
 299 discrete activity clusters. Each cluster, which consisted of 50 to 100 individual pulses,
 300 lasted approximately 2 to 3 min, separated by pauses of roughly the same duration (Fig. 4 a).
 301 There were no consistent trends of seismic amplitude with time, neither during clusters
 302 nor throughout the entire sequence. The sequence was recorded at 10:10 PST time. Seis-
 303 mic location estimates of those signal sources that were distinctive from at least three
 304 seismic stations (Fig. 3 c and d) point consistently to a region within the river channel,
 305 approximately five to ten metres upstream of station M11, with an average deviation from
 306 the independently mapped redd location of 8 m (excluding one outlier, orange dot in Fig. 3 d).

307 We also found similar results, with most of the above-mentioned characteristics of
 308 clusters of pulses, for the other potential redd-building signals (Tab. 1). These other events
 309 usually lasted several minutes. They either exhibited two to five clusters of broadband
 310 seismic pulses, each lasting less than a second, or showed a continuous though non-rhythmic
 311 occurrence of individual pulses. Those events that were suitable for estimating their source
 312 location (i.e., signals recorded by at least three stations above background noise level)
 313 all resulted from activity within the river channel. However, the location uncertainty makes
 314 any more precise links to independently mapped redd buildings unreliable. In all cases,
 315 the seismic location estimates showed higher uncertainties (e.g., 22 m on average for redd
 316 no. 1, based on signals recorded for more than 10 min on 2019-05-06 19:23 PST) than
 317 the artificial experiments (Fig. 2) and the results for redd no. 2 (Fig. 3).

318 The seismic records also exhibited signals that were not straightforward to asso-
 319 ciate with redd-building activity. One such type of signal sometimes occurred for exten-
 320 sive time periods; two hours on 20 May 18:30 PST and ten hours on 21 May 07:30 PST
 321 (Fig. 5 a). The signals show similar properties as noted above for the example event (Fig. 3):
 322 short, discrete, broad band pulses, forming clusters of up to ten pulses, which were sep-
 323 arated by several seconds of calmness. The signals were visible on at least three stations
 324 (M11, M10, M08) and could in many cases be located around redd no. 4 (Fig. 1).

325 Another outstanding, recurring signal pattern was repeatedly recorded at station
 326 M11 (Fig. 5 b). A total of 32 such events were observed throughout the instrumented

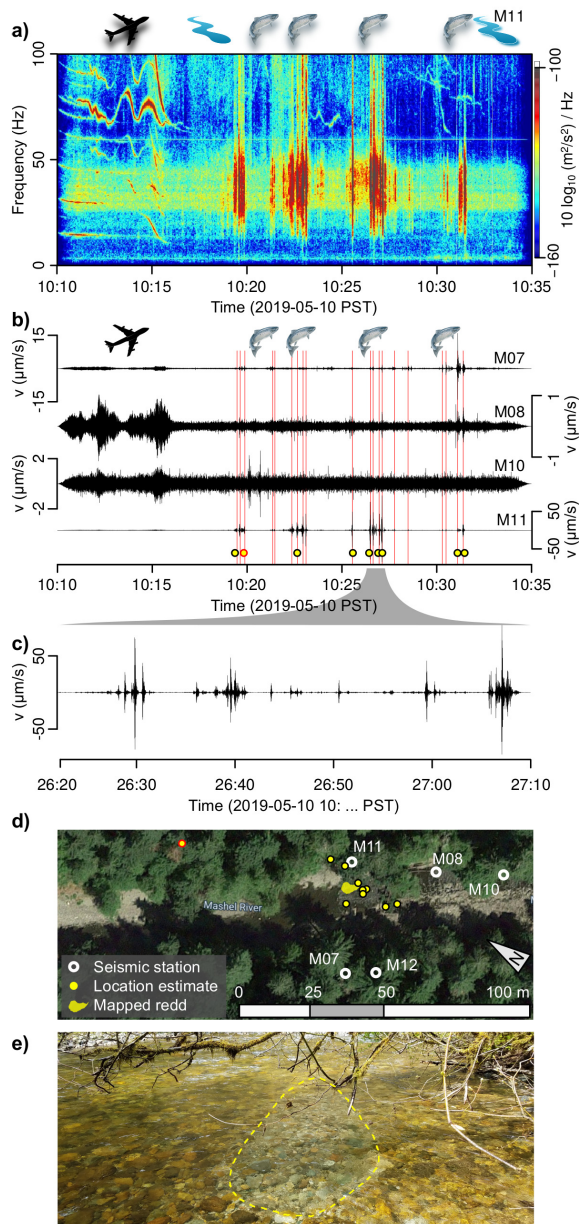


Figure 3. Seismically constrained salmonid redd activity. a) Spectrogram from station M11 showing example of plane signature as harmonic tremor (17:10–17:15 PST) and clusters of short broadband pulses (17:19–17:33 PST). Note the continuous frequency band at 30–50 Hz due to river discharge. b) Seismic waveforms of four close-by stations. Red vertical lines allow comparing the joint timing of redd-building signals at different stations. Yellow dots depict signals used for location estimates. Dot with red outline is outlier in d). c) Close-up of one redd-building cluster with a sequence of short pulses due to tail movements of steelhead. d) Seismic source location map of the signals indicated in b). e) Picture of the redd created between 8–13 May. The reworked area is indicated by the dashed yellow line.

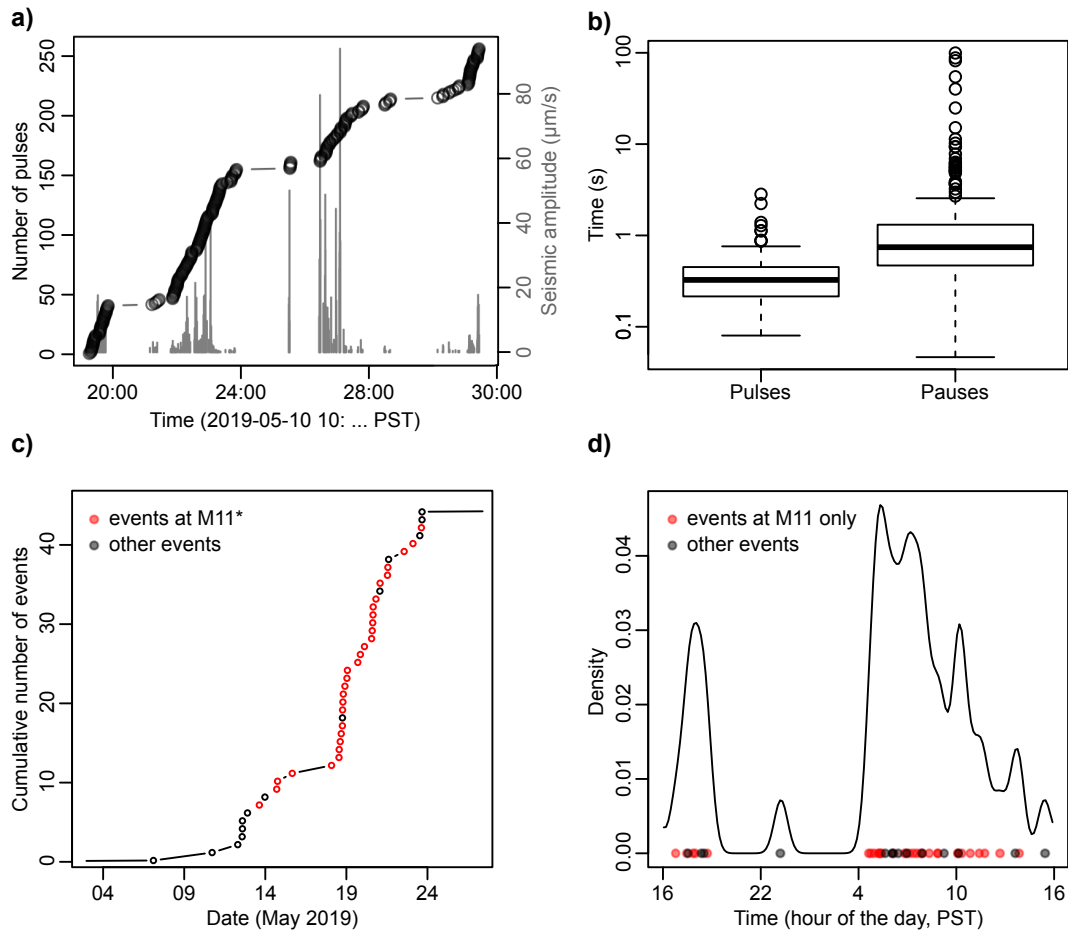


Figure 4. Characteristics of redd-building pulses and events. a) Cumulative number of individual pebble agitation pulses with time for example event from Fig. 3. b) Box plots of pulse duration and inter-pulse periods as measured at the closest seismic station. c) Cumulative number of redd-building events throughout entire survey period. d) Distribution of signal occurrence at the diurnal scale, shown as kernel density estimate plot (kernel size 16 min).

Table 1. Summary of identified seismic events (potentially) associated with redd-building activities. Seismic locations (easting and northing in UTM coordinates, signals filtered between 10 and 20 Hz throughout) are only provided when an event was clearly recorded by at least three stations. Stations with maximum seismic amplitude (A_{max}) indicate station most proximal to the potential seismic source. Index ¹ denotes events only recorded at station M11, cf. Fig. 5 b. Potential redd ID refers to IDs as shown in Fig. 1.

Event	Start time (PST)	Duration (s)	Easting (m)	Northing (m)	Station A_{max}	Redd ID
1	2019-05-06 19:23:00	600	NA	NA		1
2	2019-05-10 10:17:00	900	NA	NA	M11	2
3	2019-05-12 00:15:00	60	551217	5188989	M12	1
4	2019-05-12 06:42:35	125	551214	5189017	M11	2
5	2019-05-12 07:07:30	620	551227	5189019	M11	2
6	2019-05-12 07:10:00	1800	NA	NA	M11	2
7	2019-05-12 14:37:10	270	551220	5189006	M12	4
8	2019-05-13 08:11:00	300	NA	NA	M11 ¹	NA
9	2019-05-13 04:25:40	400	551219	5189008	M07	3
10	2019-05-14 09:54:00	300	NA	NA	M11 ¹	NA
11	2019-05-14 11:08:00	300	NA	NA	M11 ¹	NA
12	2019-05-15 08:52:00	100	NA	NA	M11 ¹	NA
13	2019-05-17 19:01:00	100	NA	NA	M11 ¹	NA
14	2019-05-18 06:02:00	300	NA	NA	M11 ¹	NA
15	2019-05-18 06:19:00	300	NA	NA	M11 ¹	NA
16	2019-05-18 07:53:00	300	NA	NA	M11 ¹	NA
17	2019-05-18 09:23:00	200	NA	NA	M11 ¹	NA
18	2019-05-18 11:06:00	400	NA	NA	M11 ¹	NA
19	2019-05-18 11:09:38	60	551228	5188999	M08	4
20	2019-05-18 11:21:00	200	NA	NA	M11 ¹	NA
21	2019-05-18 11:52:00	200	NA	NA	M11 ¹	NA
22	2019-05-18 12:25:00	200	NA	NA	M11 ¹	NA
23	2019-05-18 14:51:00	300	NA	NA	M11 ¹	NA
24	2019-05-18 17:50:00	300	NA	NA	M11 ¹	NA
25	2019-05-18 18:30:00	200	NA	NA	M11 ¹	NA
26	2019-05-19 09:54:00	200	NA	NA	M11 ¹	NA
27	2019-05-19 13:40:00	200	NA	NA	M11 ¹	NA
28	2019-05-19 19:45:00	1000	NA	NA	M11 ¹	NA
29	2019-05-20 06:19:00	300	NA	NA	M11 ¹	NA
30	2019-05-20 07:14:00	200	NA	NA	M11 ¹	NA
31	2019-05-20 07:59:00	300	NA	NA	M11 ¹	NA
32	2019-05-20 08:25:00	200	NA	NA	M11 ¹	NA
33	2019-05-20 08:38:00	600	NA	NA	M11 ¹	NA
34	2019-05-20 12:45:00	200	NA	NA	M11 ¹	NA
35	2019-05-20 18:35:00	7500	NA	NA	M12	4
36	2019-05-20 18:53:00	300	NA	NA	M11 ¹	NA
37	2019-05-21 05:50:00	900	NA	NA	M11 ¹	NA
38	2019-05-21 06:25:00	200	NA	NA	M11 ¹	NA
39	2019-05-21 07:30:00	36000	NA	NA	M12	4
40	2019-05-22 06:29:00	600	NA	NA	M11 ¹	NA
41	2019-05-23 05:42:00	600	NA	NA	M11 ¹	NA
42	2019-05-23 08:01:00	200	NA	NA	M07	3
43	2019-05-23 08:58:00	60	NA	NA	M11 ¹	NA
44	2019-05-22 19:33:00	90	551225	5188995	M08	4
45	2019-05-23 08:57:00	120	551219	5188984	M12, M11	4

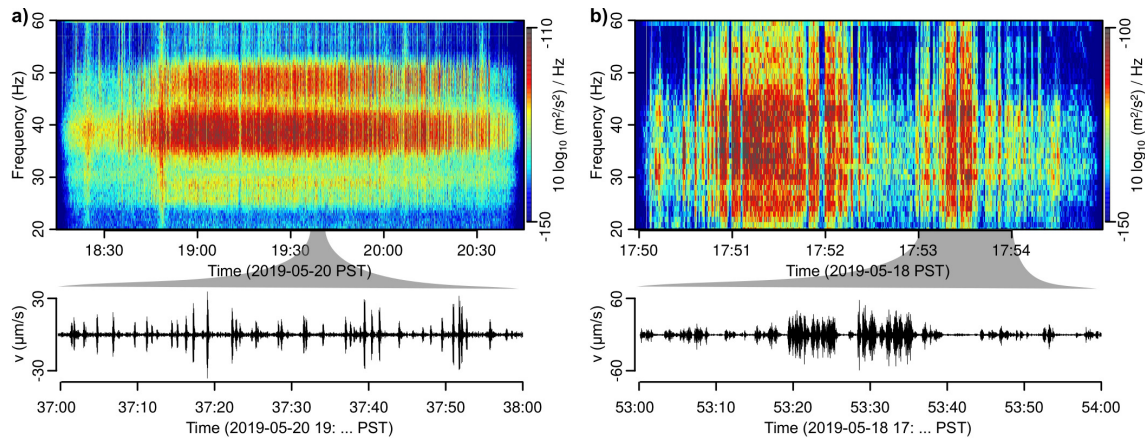


Figure 5. Seismic spectrograms and waveforms of additional signals recorded during the survey period. a) A two-hour long activity period characterised by short period 25–55 Hz pulses, most prominently recorded by station M12. b) Example of recurring activity periods with similar properties as shown in a) or Fig. 3, recorded at station M11¹.

327 period. Signal properties were in general similar to the other events from Tab. 1. How-
 328 ever, the seismic amplitudes were 20–30 % weaker than the signals from Fig. 3; although
 329 the signals were clearly visible at station M11, the signals were not distinct from back-
 330 ground noise levels at the other stations. Accordingly, it was not possible to estimate
 331 the location of their sources.

332 5 Discussion

333 5.1 Proof of concept

334 We demonstrate the potential of a seismic approach for identifying the spatial and
 335 temporal patterns of redd-building activity using two independent approaches – com-
 336 paring seismic data collected during construction of man-made artificial redds and dur-
 337 ing construction of redds by a native, wild salmonids. The artificially-induced signals (man-
 338 made redds, Fig. 2) showed major spectral overlap with the frequency window of the river-
 339 induced seismic signature (Dietze, Lagarde, et al., 2019; Gimbert et al., 2014) and only
 340 type 1 and 2 agitation yielded a seismic signal sufficiently different from background noise
 341 (Fig. 2 a). This complements our work demonstrating the ability of our seismic approach
 342 to detect four redds created by steelhead in the natural setting.

343 The links between seismic data and manually mapped redds are based on both joint
 344 time windows, and seismic source location estimates matching with mapped locations.
 345 These links, although robust, open up room for interpretation, predominantly because
 346 of the large mapping time intervals, and to a lesser degree because of the spatial uncer-
 347 tainty of the seismic location estimate. Thus, future work should be focused on further
 348 validation of seismic signal inferences of salmonid redd construction over a variety of species
 349 and spatial/temporal scales. Whenever a location for the events from Tab. 1 was possi-
 350 ble, it pointed at a seismic source inside the river. This already rules out any poten-
 351 tial terrestrial causes for the measured signals. Although signals such as those from Fig. 3
 352 could in principle be generated by animals like woodpeckers, the location constraint does
 353 not support such a hypothesis. Likewise, spatially mobile seismic sources, such as per-
 354 sons wading the river or animals passing a seismic station outside the river, would stand
 355 in conflict with the stable seismic location results and the lack of systematic increases
 and decreases of seismic amplitudes at a given seismic station. Other signals from in-

side the river but not related to fish activity might be river bedload transport. However, studies from rivers in different settings, from sand- to gravel- and even boulder-beds channels and from flash-flood dominated to continuously active (Polvi et al., in review; Dietze, Lagarde, et al., 2019; Dietze, Gimbert, et al., 2019; Burtin et al., 2016) consistently showed that bedload transport results in overall increased amplitudes of the seismic signals of certain frequencies and not in the emergence of erratic short seismic pulses. Furthermore, the seismic spectrogram of the entire study period (Fig. 1 b) did not show any indications of sustained bedload movement during the rain-driven high flow events. Finally, rain drop impacts can be excluded as an explanation of the seismic pulses from Fig. 3 or Fig. 5 because these seismic pulses (which were recorded by at least three stations) provided location estimates within the river channel. Thus, we propose that the seismic signals we report here were indeed caused by biotic activity within the river channel, more specifically by steelhead actively redistributing river bed material.

The redd-construction signal example illustrated in Fig. 3 showed that redd-building signals could be recorded up to a distance of at least 50 m (distance between redd no. 1 and station M10) and yield very clear signals (signal-to-noise-ratio > 40) at distances of less than 10 m (e.g., M07, M11). The artificially-induced signals that generated sufficient seismic energy could be located, using the migration technique, with deviations of less than five metres on average. This sets the location precision baseline for any other internal river location exercises. While high location precision may be less important when the goal is simply to detect when, how and how long redd building activity occurs, this feature becomes essential when the goal is to map out individual redd buildings and their evolution with time. Given a river width of 25 m and an average distance between four mapped redds of $20.4^{+7.7}_{-5.3}$ m, the seismic method allows for sufficient accuracy to discriminate between different redds; however, this is a tentative estimate based on the small number of samples. The location estimate could be improved in subsequent surveys by i) using a denser station network (less than 10 m station spacing), ii) sampling the signals by more than 400 Hz, a recording frequency which allows no more than approximately one meter accuracy in this environment when using the arrival time-based migration approach to locating seismic sources, and iii) reducing the noise background, for example by burying the sensors. A drawback of this study design was that the geophones were not buried but installed on the ground. This resulted in many spurious event detections that ultimately turned out to be plane crossings (Fig. 3 a). Likewise, stations more than 50 m away from the banks (results not shown) did not record any of the signals registered by the network compartments close to the stream.

5.2 Redd building anatomy

For over a century, biologists and fisheries managers have contemplated the spawning behaviour of salmonids. For species that spawn more than once, and therefore benefit from surviving post spawning, the mating behaviour and associated redd-building activities are often elusive and thought to take place in the evening hours. However, a small number of studies have documented spawning of steelhead and other species occurring during daylight hours. The current study sheds light on this data gap and suggests that the majority of spawning for steelhead trout takes place during daylight hours and is focused around the crepuscular period. For steelhead, there is likely a trade-off between attracting a mate, avoiding predation and metabolic demands associated with spawning that may be tied to stream temperature. Needham and Taft (1934) recorded short periods of digging prior to spawning followed by additional short periods of digging to bury recently expelled and fertilized eggs. This was then repeated one or more times at the same site across multiple days (and possibly nights). Our passively recorded measurements of gravel transport associated with spawning are in agreement with the observations of Needham and Taft (1934) and take the spawning description one step further by describing the event at a much finer scale and highlighting the importance of the crepuscular period for spawning. Specifically, at the diurnal scale, redd-building

410 activity in the current study showed a distinct pattern (Fig. 4 d). The majority of redd-
 411 building signals occurred between early morning and noon local time (i.e., 05–13 PST),
 412 with a focused onset and a slowly receding rate. A secondary cluster emerges in the evening
 413 (i.e., 17–20 PST). There are no significant differences between the repeated events only
 414 recorded at station M11 (Fig. 5 b) and the other events. We interpret this diurnal pat-
 415 tern as preferred fish activity during daytime but avoiding the middle of the day with
 416 highest temperatures and direct sunlight. It remains unclear if these long activity pe-
 417 riods, lasting several hours, are typical for steelhead across the range. With a protracted
 418 spawning period occurring over more than 4 months, steelhead lend themselves to ad-
 419 ditional work that collects information across a greater number of spawners. Addition-
 420 ally, focusing this work on semelparous species that have a less flexible spawning win-
 421 dow may provide insight into how different life history strategies shape spawning behaviour.

422 This work resulted in a dramatic improvement in the understanding of spawning
 423 behaviour of steelhead and paves the way for improved tools to monitor salmonids and
 424 the effects they have on the hydraulic and sedimentological characteristics of a stream.
 425 In addition, this first attempt at applying seismic monitoring to fisheries management
 426 highlight important next steps to fine tune this work. The duration of a steelhead spawn-
 427 ing event in this study averaged 6 days. About 90 % of spawning took place during day-
 428 light hours (07–18 PST), and 60 % of spawning behaviour took place in morning hours
 429 before noon (Fig. 4 c).

430 It has been shown that the process of building a redd can take several days for steel-
 431 head, including both the stage before and the stage after the spawning phase (Needham
 432 & Taft, 1934; Burner, 1951; Fuchs & Caudill, 2019). Thus, one single sequence of pulses
 433 lasting 10–20 min will certainly not be enough to create a proper redd, and it is to be
 434 expected that there must be additional and extensive seismic redd-building signals. For
 435 redd no. 2 (Fig. 1 a, Tab. 1), there were four discrete pulse sequences with a location
 436 matching a surveyed redd. In addition, there is the day-long, repeated occurrence of sev-
 437 eral minute-long sequences that were only visible at station M11 which is closest to redd
 438 no. 2. In principle, these findings could be interpreted as the seismic signature of the full
 439 redd-building, spawning and redd-finalisation process, in agreement with previous data
 440 (Burner, 1951; Gottesfeld et al., 2004). Particularly given that during an 11-day period
 441 we were able to detect indications of activity located at or near all of the independently
 442 mapped redd locations. However, without more robust location information, this remains
 443 tentative, especially for redd locations so close together in space. For instance, redds no.
 444 3 and no. 4 could perhaps be linked with several repeated seismic activity clusters be-
 445 tween 12 and 23 May given the close proximity where these spawning events took place.
 446 However, a robust seismic location estimate would be needed to properly support this
 447 interpretation and would be recommended for future work.

448 5.3 Perspectives

449 Based on previous experience with seismic sensors to detect and quantify fluvial
 450 sediment transport dynamics (Dietze, Lagarde, et al., 2019; Polvi et al., in review), the
 451 boundary conditions for a functional seismic network were determined. Given the gen-
 452 eral success of the seismic approach to detect and quantitatively describe the process of
 453 redd building, we propose objectives and strategies of subsequent research in that direc-
 454 tion. 1) A longer instrumentation time is required to survey the full spawning season.
 455 This requires rethinking logistics of power provision and station maintenance. 2) The
 456 network layout, which was designed in this study to account for a hitherto unknown type
 457 of seismic source, should be optimised. At a minimum, this means that there is no need
 458 to deploy stations far away from the banks. Rather, stations should be set up close to
 459 the banks, at distances of less than 10 m from each other. In addition, the sensors should
 460 be deployed below the surface to reduce signal contamination by sources such as air traf-
 461 fic and weather phenomena. 3) An active seismic survey covering the entire reach to be

462 monitored proved essential to constrain the seismic wave velocity, required for robust source
463 location estimates. Further seismic details can be provided by estimating the seismic en-
464 ergy emitted by the fish activity, which can be interpreted as an equivalent of kinetic en-
465 ergy. For this step, one could use existing laws to relate seismic amplitudes as recorded
466 by several stations to the amplitude at the located source (e.g. Burtin et al., 2016). 4)
467 Fundamentally, a future study would benefit from more independent confirmation data.
468 These could be provided by time lapse imagery on sub areas of the surveyed reach, de-
469 tailed mapping of (previously seismically detected and located) redds to check to which
470 extent these redds have been modified between mapping surveys, and how much mate-
471 rial has been mobilised and redistributed. Finally, 5) utilisation of automatic approaches
472 to redd building event detection would be essential to reduce the amount of manual work-
473 load. Machine learning solutions open promising avenues in this regard, especially since
474 the unique properties of the signals identified by us (rhythmic short pulses of similar spec-
475 tral patterns from inside the stream) could be easily translated into features, required
476 for seismic event classification (e.g. Hibert et al., 2017).

477 6 Conclusions

478 We successfully tested a new method to survey a fundamentally important phe-
479 nomenon in river ecology as well as fluvial geomorphology: salmonid redd-building ac-
480 tivity in gravel-bed rivers. The seismic approach can be highly complementary to the
481 range of methods classically employed. Furthermore, in many regions, visual surveying
482 of redds is not possible because of, for example, low visibility due to high turbidity or
483 humic water, difficult to distinguish redds due to dark-coloured sediment, and deep wa-
484 ter. Therefore, the seismic method would allow data on redd-building to be collected for
485 the first time in many regions (e.g., northern Europe). It also allows for continuous mon-
486 itoring regardless of environmental conditions, providing high-resolution insight into the
487 dynamics of redd-building, from minute-long excavation activity clusters to the kinet-
488 ics of individual pebble agitation pulses, and it allows estimates of the location of these
489 individual pulses. Based on these detailed data, we found that excavation appears to oc-
490 cur preferentially during daytime, starting in the early morning, with a pause in the mid-
491 dle of the day and another peak in the late afternoon, with almost no activity during the
492 night. Individual activity pulses of bed material agitation, lasting less than a second and
493 forming clusters of 50 to 100 pulses are separated by minute-long pauses – a pattern that
494 is in agreement with results from other studies on the redd-building process. The deci-
495 sively generic network design showed that in future studies, stations should be deployed
496 linearly along both banks in order to optimise the detection and location quality.

497 In addition to learning more about spawning behavior, this study can open doors
498 to understanding geomorphic change by salmonids. While seasonal sediment transport
499 by salmonids has been quantified, with seismological methods, we can make more pre-
500 cise calculations of sediment flux (Dietze et al. 2019), clearly partitioned between flu-
501 vial and biological processes. Seismic location estimates of redd-building signals can al-
502 low a better understanding of potential sub-reach morphologic effects of spawning. More-
503 over, the approach would not be restricted to redd building activity, but could be gen-
504 eralised to further biological agents that actively move sediment particles, given that the
505 seismic signature of their activity is distinct enough to be detected and attributed to the
506 animal under focus. Thus our results provide a methodology with the potential to ad-
507 dress large unanswered questions about ecosystem engineers and bioturbators (Polvi &
508 Sarneel, 2018), including effects on smaller and larger spatial scales than traditionally
509 measured.

510 Acknowledgments

511 We thank the following for assistance in the field, with set-up, geomorphic measurements,
512 and redd surveys: Annika Holmgren and Gustav Hellström with the Swedish University

513 of Agricultural Sciences and Gabe Madel, Riley Freeman and Steve Boessow with the
 514 Washington Department of Fish and Wildlife. We thank the Geophysical Instrument Pool
 515 Potsdam (GIPP) for provision of the seismic stations.

516 7 Data availability statement

517 The raw seismic data are available under the DOI 10.5880/GFZ.4.6.2020.004 (Dietze
 518 et al., 2020). The SI contain all code and information necessary to reproduce the results
 519 of this study. All other data is available from the public resources as referenced in the
 520 text.

521 References

- 522 Allen, R. (1982). Automatic phase pickers: Their present use and future prospects.
 523 *Bulletin of the Seismological Society of America*, 72, S225–S242.
- 524 Berejikian, B., Johnson, T., Endicott, R., & Lee-Waltermire, J. (2008). In-
 525 creases in steelhead (*oncorhynchus mykiss*) redd abundance resulting from
 526 two conservation hatchery strategies in the hamma hamma river, washington.
 527 *Canadian Journal of Fisheries and Aquatic Sciences*, 65(4), 754–764. doi:
 528 10.1139/F08-014
- 529 Bourbie, T., Coussy, O., & Zinszner, B. (1987). *Acoustics of porous media*. Gulf
 530 Publishing Company.
- 531 Burner, C. J. (1951). *Characteristics of spawning nests of columbia river salmon*. US
 532 Department of the Interior.
- 533 Burtin, A., Hovius, N., & Turowski, J. M. (2016). Seismic monitoring of torrential
 534 and fluvial processes. *Earth Surface Dynamics*, 4, 285–307. doi: 10.5194/esurf
 535 -4-285-2016
- 536 de Oliveira Frascá, M. H. B., & Del Lama, E. A. (2018). Biological weathering. In
 537 P. T. Bobrowsky & B. Marker (Eds.), *Encyclopedia of engineering geology* (pp.
 538 61–62). Springer International Publishing. doi: 10.1007/978-3-319-73568-9_29
- 539 Dietze, M. (2018a). 'eseis' – an R software toolbox for environmental seismology. v.
 540 0.4.0. GFZ Data services. doi: <http://doi.org/10.5880/GFZ.5.1.2018.001>
- 541 Dietze, M. (2018b). The R package "eseis" – a software toolbox for environmen-
 542 tal seismology. *Earth Surface Dynamics*, 6, 669–686. doi: 10.5194/esurf-6-669
 543 -2018
- 544 Dietze, M., Gimbert, F., Turowski, J., Stark, K., Cadol, D., & Laronne, J. (2019).
 545 The seismic view on sediment laden ephemeral flows – modelling of ground
 546 motion data for fluid and bedload dynamics in the arroyo de los piños [Com-
 547 puter software manual]. Retrieved from [http://micha-dietze.de/pages/
 548 publications/other/Dietze_et_al_2019b.pdf](http://micha-dietze.de/pages/publications/other/Dietze_et_al_2019b.pdf) (Paper to SEDHYD confer-
 549 ence)
- 550 Dietze, M., Lagarde, S., Halfi, E., Laronne, J. B., & Turowski, J. M. (2019). Joint
 551 sensing of bedload flux and water depth by seismic data inversion. *Water Re-
 552 sources Research*, 55(11), 9892–9904. doi: 10.1029/2019WR026072
- 553 Dietze, M., Losee, J., Polvi, L., & Palm, D. (2020). *Seismic data from a project on
 554 monitoring of salmonid nest building, Mashel River, USA, v. 0.1.0*. GFZ Data
 555 services. doi: <http://doi.org/10.5880/GFZ.4.6.2020.004>
- 556 Dietze, M., Mohadjer, S., Turowski, J., Ehlers, T., & Hovius, N. (2017). Validity,
 557 precision and limitations of seismic rockfall monitoring. *Earth Surface Dynam-
 558 ics*, 2017, 1–23. doi: 10.5194/esurf-2017-12
- 559 Field-Dodgson, M. (1987). The effect of salmon redd excavation on stream substrate
 560 and benthic community of two salmon spawning streams in canterbury, new
 561 zealand. *Hydrobiologia*, 154, 3–11. doi: 10.1007/BF00026826
- 562 Fremier, A. K., Yanites, B. J., & Yager, E. M. (2018). Sex that moves moun-
 563 tains: The influence of spawning fish on river profiles over geologic timescales.

- 564 *Geomorphology*, 305, 163 - 172. (Resilience and Bio-Geomorphic Systems
565 Proceedings of the 48th Binghamton Geomorphology Symposium) doi:
566 <https://doi.org/10.1016/j.geomorph.2017.09.033>
- 567 Fuchs, N., & Caudill, C. (2019). Classifying and inferring behaviors using real-
568 time acceleration biotelemetry in reproductive steelhead trout (*Oncorhynchus*
569 *mykiss*). *Ecology and Evolution*, 9, 11329–11343. doi: 10.1002/ece3.5634
- 570 Gallagher, S., & Gallagher, C. (2005). Discrimination of chinook salmon, coho
571 salmon, and steelhead redds and evaluation of the use of redd data for es-
572 timating escapement in several unregulated streams in northern california.
573 *North American Journal of Fisheries Management*, 25(1), 284-300. doi:
574 10.1577/M04-016.1
- 575 Gallagher, S. P., Hahn, P. K. J., & Johnson, D. H. (2007). Redd counts. In
576 D. H. Johnson et al. (Eds.), *Salmonid field protocols handbook: techniques*
577 *for assessing status and trends in salmon and trout populations* (pp. 197–234).
578 Bethesda, Maryland: American Fisheries Society.
- 579 Gimbert, F., Tsai, V., & Lamb, M. (2014). A physical model for seismic noise gener-
580 ation by turbulent flow in rivers. *Journal of Geophysical Research*, 119, 2209–
581 2238. doi: 10.1002/2014JF003201
- 582 Gottesfeld, A. S., Hassan, M. A., Tunnicliffe, J. F., & Poirier, R. W. (2004). Sed-
583 iment dispersion in salmon spawning streams: The influence of floods and
584 salmon redd construction1. *JAWRA Journal of the American Water Resources*
585 *Association*, 40(4), 1071-1086. doi: 10.1111/j.1752-1688.2004.tb01068.x
- 586 Harvey, G. L., Henshaw, A. J., Brasington, J., & England, J. (2019). Burrowing in-
587 vasive species: An unquantified erosion risk at the aquatic-terrestrial interface.
588 *Reviews of Geophysics*, 57(3), 1018-1036. doi: 10.1029/2018RG000635
- 589 Hassan, M. A., Gottesfeld, A. S., Montgomery, D. R., Tunnicliffe, J. F., Clarke,
590 G. K. C., Wynn, G., ... Macdonald, S. J. (2008). Salmon-driven bed load
591 transport and bed morphology in mountain streams. *Geophysical Research*
592 *Letters*, 35(4). doi: 10.1029/2007GL032997
- 593 Heimann, S., Kriegerowski, M., Isken, M., Cesca, S., Daout, S., Grigoli, F., ...
594 Dahm, T. (2017). *Pyrocko - an open-source seismology toolbox and library*.
595 GFZ Data services. doi: <http://doi.org/10.5880/GFZ.2.1.2017.001>
- 596 Hibert, C., Provost, F., Malet, J.-P., Maggi, A., Stumpf, A., & Ferrazzini, V. (2017).
597 Automatic identification of rockfalls and volcano-tectonic earthquakes at the
598 piton de la fournaise volcano using a random forest algorithm. *J. Volcanol.*
599 *Geotherm. Res.*, 340, 130-140. doi: 10.1016/j.jvolgeores.2017.04.015
- 600 IRIS. (2017). *Incorporated research institutions for seismology – using sac*. Available
601 at ds.iris.edu/ (2017/12/16).
- 602 Losee, J. P., Phillips, L., & Young, W. C. (2016). Spawn timing and redd mor-
603 phology of anadromous coastal cutthroat trout *oncorhynchus clarkii clarkii*
604 in a tributary of south puget sound, washington. *North American Journal of*
605 *Fisheries Management*, 36(2), 375-384. doi: 10.1080/02755947.2015.1129001
- 606 Madel, G., & Losee, J. (2016). *Research and monitoring of adult Oncorhynchus*
607 *mykiss in the nisqually river* (Tech. Rep.). Washington Department of Fish
608 and Wildlife.
- 609 Needham, P., & Taft, A. (1934). Observations on the spawning of steelhead trout.
610 *Trans. Amer. Fish Soc.*, 64.
- 611 NOAA. (2020). *National weather forecast service*. [https://w2.weather.gov/](https://w2.weather.gov/climate/xmacis.php?wfo=sew)
612 [climate/xmacis.php?wfo=sew](https://w2.weather.gov/climate/xmacis.php?wfo=sew). (Accessed: 2020-03-10)
- 613 Phillips, J., Samonil, P., Pawlik, ., Trochta, J., & Dank, P. (2016, 10). Domination
614 of hillslope denudation by tree uprooting in an old-growth forest. *Geomorphol-*
615 *ogy*, 276. doi: 10.1016/j.geomorph.2016.10.006
- 616 Polvi, L., Dietze, M., Lotsari, E., Turowski, J., & Lind, L. (in review). Seismic
617 monitoring of a subarctic river: seasonal variations in hydraulics, sediment
618 transport and ice dynamics. in review. *Journal of Geophysical Research: Earth*

*Surface.*619
620
621
622
623
624
625
626
627
628
629
630
631
632
633
634
635
636
637
638
639
640
641
642
643
644

Polvi, L., & Sarneel, J. (2018). Ecosystem engineers in rivers: An introduction to how and where organisms create positive biogeomorphic feedbacks. *WIREs Water*, 5(2), e1271. doi: 10.1002/wat2.1271

Quinn, T. (2018). *The behavior and ecology of pacific salmon and trout*. University of Washington Press.

Rand, P. S., & Fukushima, M. (2014). Estimating the size of the spawning population and evaluating environmental controls on migration for a critically endangered asian salmonid, sakhalin taimen. *Global Ecology and Conservation*, 2, 214 - 225. doi: <https://doi.org/10.1016/j.gecco.2014.09.007>

Rennie, C., & Millar, R. (2000). Spatial variability of streambed scour and fill: A comparison of scour depth in chum salmon (*oncorhynchus keta*) redds and adjacent bed. *Canadian Journal of Fish and Aquatic Science*, 57, 928–938. doi: 10.1016/j.geomorph.2016.10.006

Schmandt, B., Gaeuman, D., Stewart, R., Hansen, S., Tsai, V., & Smith, J. (2017). Seismic array constraints on reach-scale bedload transport. *Geology*, 45, 299–302. doi: 10.1130/G38639.1

Turowski, J. M., Dietze, M., Schöpa, A., Burtin, A., & Hovius, N. (2016). Vom flüstern, raunen und grollen der landschaft. seismische methoden in der geomorphologie. *System Erde*, 6, 56–61. doi: 10.2312/GFZ.syserde.06.01.9

USGS. (2020). *National water information system: Web interface*. https://waterdata.usgs.gov/nwis/uv?site_no=12087000. (Accessed: 2020-03-10)

Viles, H. (1988). *Biogeomorphology*. Blackwell.

Welch, P. (1967). The use of fast Fourier transform for the estimation of power spectra: A method based on time averaging over short, modified periodograms. *IEEE Transactions on Audio and Electroacoustics*, 15, 70–73.